Journal of Inorganic Biochemistry 164 (2016) 99–109

Contents lists available at ScienceDirect

Journal of Inorganic Biochemistry

journal homepage: www.elsevier.com/locate/jinorgbio

Role of subcellular calcium redistribution in regulating apoptosis and autophagy in cadmium-exposed primary rat proximal tubular cells

Fei Liu [a], Zi-Fa Li [b], Zhen-Yong Wang [a], Lin Wang [a,*]

[a] College of Animal Science and Veterinary Medicine, Shandong Agricultural University, Daizong Road No. 61, Tai'an 271018, People's Republic of China
[b] Laboratory Animal Center of Shandong University of Traditional Chinese Medicine, Jinan 250355, People's Republic of China

ARTICLE INFO

Article history:
Received 13 June 2016
Received in revised form 30 August 2016
Accepted 13 September 2016
Available online 14 September 2016

Keywords:
Cadmium
Apoptosis
Autophagy
Endoplasmic reticulum
Cytosolic calcium overload
Proximal tubular cells

ABSTRACT

Ca^{2+} signaling plays a vital role in regulating apoptosis and autophagy. We previously proved that cytosolic Ca^{2+} overload is involved in cadmium (Cd)-induced apoptosis in rat proximal tubular (rPT) cells, but the source of elevated cytosolic Ca^{2+} concentration ($[Ca^{2+}]_c$) and the effect of potential subcellular Ca^{2+} redistribution on apoptosis and autophagy remain to be elucidated. Firstly, data showed that Cd-induced elevation of $[Ca^{2+}]_c$ was primarily generated intracellularly. Moreover, elevations of $[Ca^{2+}]_c$ and mitochondrial Ca^{2+} concentration ($[Ca^{2+}]_{mit}$) with depletion of endoplasmic reticulum (ER) Ca^{2+} levels ($[Ca^{2+}]_{ER}$) were revealed in Cd-treated rPT cells, but this subcellular Ca^{2+} redistribution was significantly suppressed by 2-Aminoethoxydiphenyl borate (2-APB). Elevated inositol 1,4,5-trisphosphate (IP_3) levels with up-regulated IP_3 receptor (IP_3R) protein levels were shown in Cd-exposed cells, confirming that IP_3R-mediated ER Ca^{2+} release results in the elevation of $[Ca^{2+}]_c$. Up-regulated sequestosome 1 (p62) protein levels and autophagic flux assay demonstrated that Cd impaired autophagic degradation, while *N*-acetylcysteine (NAC) markedly attenuated Cd-induced p62 and microtubule-associated protein 1 light chain 3-II (LC3-II) accumulation, implying that the inhibition of autophagic flux was due to oxidative stress. Furthermore, pharmacological modulation of $[Ca^{2+}]_c$ with 1,2-Bis (2-aminophenoxy) ethane-*N*,*N*,*N*′,*N*′-tetraacetic acid acetoxymethyl ester (BAPTA-AM) and 2-APB alleviated Cd-mediated apoptosis, inhibition of autophagic degradation and subsequent cytotoxicity, while thapsigargin (TG) had the opposite regulatory effect on them. In summary, cytosolic calcium overload originated from IP_3R-mediated ER Ca^{2+} release has a negative impact on Cd nephrotoxicity through its promotion of apoptosis and inhibition of autophagic flux.

1. Introduction

Cadmium (Cd) is a widespread heavy metal pollutant in the environment due to its extensive use in various anthropogenic and industrial activities. The main routes of human exposure to Cd are via inhalation of Cd-contaminated dust particles (aerosols) or cigarette smoke and ingestion of contaminated water and food [1]. As a nonessential element, it exerts toxic effects on multiple organs in mammals and has been classified as a human carcinogen by the International Agency for Research on Cancer [2]. With the chronic, low-level Cd exposure that are common in humans, kidney is the most sensitive target organs of toxicity [3], where Cd accumulates primarily in the proximal tubule of the nephron [4], resulting in a generalized reabsorptive dysfunction characterized by polyuria and low molecular weight proteinuria [5]. Primary cultures can better represent the live tissue than permanent cell lines, which are ideal for in vitro toxicology studies. Therefore, primary cultures of rPT cells were established to investigate low-level Cd-induced nephrotoxicity in this study.

Autophagy is a self-digesting mechanism responsible for the degradation and recycling of damaged organelles, misfolded proteins, and other macromolecules in lysosomes, which plays a crucial role in cellular homeostasis and adaptation to adverse stress conditions [6]. In mammals, the net amount of LC3-II is a key hallmark for monitoring autophagy; moreover, analysis of autophagic flux is more reliable to represent the dynamic process of autophagy [7]. There is a growing amount of evidence that dysregulation of the autophagic pathway is implicated in the pathogenesis of kidney aging and in several renal diseases such as acute kidney injury, polycystic kidney disease, diabetic nephropathy, obstructive nephropathy, focal and segmental glomerulosclerosis, and potentially other kidney disease [8]. It has also been demonstrated that blockade of the autophagic flux can induce cell death in various types of cells [9]. Proximal tubular is the target site for Cd-induced renal damage, which prompts us to investigate the role of autophagy in Cd-exposed rPT cells.

Generally, mechanism of Cd nephrotoxicity is ascribed to the action of oxidative stress and apoptosis [10–12]. Our research group found that

* Corresponding author.
E-mail address: wanglin2013@sdau.edu.cn (L. Wang).

http://dx.doi.org/10.1016/j.jinorgbio.2016.09.005
0162-0134/

oxidative stress-mediated apoptotic death played a key role in Cd-induced nephrotoxicity in vitro; moreover, it is important to note that intracellular Ca^{2+} overload is involved in this process [13]. The cytosolic Ca^{2+} concentration ($[Ca^{2+}]_c$) is tightly controlled by intracellular calcium stores such as mitochondria and ER, which are also the main sites of apoptotic and autophagic regulation [14]. Inositol 1,4,5-trisphosphate (IP_3) is an important secondary messenger in cell signaling [15], and cytosolic signals caused by Ca^{2+} release from the ER through IP_3 receptor (IP_3R) Ca^{2+} channels regulate numerous cellular functions [16]. Ca^{2+} release from the ER is known to be apoptogenic, which ultimately leads to $[Ca^{2+}]_c$ elevation, and associated with apoptotic death and autophagy inhibition [14,17]. However, several critical items remain unclear regarding the crosstalk between apoptosis and autophagy in response to $[Ca^{2+}]_c$ elevation during Cd nephrotoxicity. Where does Cd-induced $[Ca^{2+}]_c$ elevation originate from, intracellularly or extracellularly? What is the role of ER Ca^{2+} stores in the process of Cd-induced subcellular calcium redistribution? What are the eventual functions of autophagy in Cd-induced cytotoxicity of rPT cells? Can $[Ca^{2+}]_c$ elevation serve as a link mediating the apoptosis and autophagy in Cd-exposed rPT cells? This study will offer further evidences to clarify these questions and investigate the regulatory effect of $[Ca^{2+}]_c$ elevation on apoptosis and autophagy in Cd-exposed rPT cells.

2. Materials and methods

2.1. Chemicals and antibodies

All chemicals were of highest grade purity available. 2-Aminoethoxydiphenyl borate (2-APB) and 1,2-Bis (2-aminophenoxy) ethane-*N*,*N*,*N*′,*N*′-tetraacetic acid acetoxymethyl ester (BAPTA-AM) were from Tocris Bioscience (Bristol, UK). Thapsigargin (TG) was from Thermo Fisher Scientific Inc. Dihydro-Rhod-2-AM, Mag-Fluo-4-AM and *N*,*N*,*N*′,*N*′-tetrakis-(2-pyridylmethyl) ethylenediamine (TPEN) were bought from Molecular Probes (Eugene, OR, USA). Cell Counting Kit-8 (CCK-8, CK04-3000), Pluronic F-127 and Fluo-4-AM were obtained from Dojindo Laboratories (Tokyo, Japan). Annexin V-FITC apoptosis detection kit was from Pharmingen (Becton Dickinson Company, USA). Five primary antibodies were used: inositol 1,4,5-triphosphate receptor 1 (IP_3R-1) antibody (Sigma, SAB5200080), inositol 1,4,5-triphosphate receptor 2 (IP_3R-2) antibody (Novus Biologicals, NB100-2466), anti-p62/SQSTM1 antibody (Sigma, P0067), anti-LC3B (Sigma, L7543) and anti-β-actin antibody (Sigma, A5441). Secondary antibodies were conjugated to horseradish peroxidase (Jackson Immuno Research, 705-505-303 and 111-006-062). Calcium-free medium (CFM) was a 1:1 (v/v) mixture of Ca^{2+}-free HAM's F12 (US Biological, N8542-10) and Ca^{2+}-free DMEM high glucose (Invitrogen, 21068-028) supplemented with 1.5 mM glutamine, 22 mM sodium bicarbonate, 12.5 mM HEPES, 10 μg/mL insulin and 5.5 μg/mL transferin. Bicinchonininc acid (BCA) protein assay kit and enhanced chemiluminescence (ECL) kit were obtained from Sangon Biotech Co., Ltd. (Shanghai, China). Cadmium acetate ($CdAc_2$), propidium iodide (PI), DMEM-F_{12} (1:1) medium, Hoechst 33258, *N*-acetylcysteine (NAC), sodium borohydride ($NaBH_4$), chloroquine diphosphate salt (CQ) and all other chemicals were purchased from Sigma-Aldrich, USA.

2.2. Cell culture and Cd treatment

All procedures followed the ethics guidelines and were approved by the Animal Care and Use Committee of Shandong Agricultural University. Isolation, identification and culture of Sprague-Dawley rPT cells were as previously described [18]. Based on the doses of Cd in our previous study [13], 2.5 μM Cd was applied in this study. BAPTA-AM, TG and 2-APB were dissolved in DMSO to make the stock solution, filtered and stored at −20 °C, then diluted to work solution prior to use. The final concentration of DMSO was <0.1% and 0.1% DMSO has no effect on Ca^{2+} signaling and cell viability [19]. $CdAc_2$, CQ and NAC were dissolved in sterile ultrapure water.

2.3. Measurement of cytosolic Ca^{2+} concentration ($[Ca^{2+}]_c$)

Changes of $[Ca^{2+}]_c$ were assessed by flow cytometry. The first subculture was refreshed with CFM (Ca^{2+}-free DMEM-F_{12} as described above) when it reached around 80% confluence. After 20 min adaptation, cells were exposed to 2.5 μM Cd for a time range of 0 h, 1 h and 2 h, respectively. Following the treatment (0 h, 1 h and 2 h), harvested cells were incubated with 0.5 mM TPEN at 37 °C for 10 min, loaded with 1 μM Fluo-4-AM (containing 0.02% Pluronic F-127) for 30 min in dark at 37 °C, and then washed with D-Hank's solution. Intracellular $[Ca^{2+}]_c$ levels were represented with fluorescent intensity (FL-1, 530 nm) of 10,000 cells on flow cytometer. Meanwhile, changes of $[Ca^{2+}]_c$ were determined in 2.5 μM Cd-treated rPT cells cultured in regular DMEM-F_{12} medium (containing Ca^{2+}) using the same detection method.

2.4. Determination of mitochondrial Ca^{2+} concentration ($[Ca^{2+}]_{mit}$)

Our previous study has confirmed the specificity of dihydro-Rhod-2-AM to detect $[Ca^{2+}]_{mit}$ [20]. In this study, changes of $[Ca^{2+}]_{mit}$ were analyzed by flow cytometry. So Rhod-2-AM was first incubated with particular amounts of $NaBH_4$ for 10 min at 4 °C to produce dihydro-Rhod-2-AM according to the manufacturer's manual as described previously [21]. Cells were treated with TPEN, followed by incubating with 5 μM dihydro-Rhod-2-AM and 0.02% (w/v) Pluronic F-127 for 30 min at 37 °C in dark. $[Ca^{2+}]_{mit}$ was measured by the fluorescence intensity (FL-1, 585 nm) of 10,000 cells on flow cytometer.

2.5. Analysis of endoplasmic reticulum Ca^{2+} levels ($[Ca^{2+}]_{ER}$)

It has been verified that Mag-Fluo-4-AM was selectively labelled on ER, making its specificity for measuring $[Ca^{2+}]_{ER}$ [20]. After corresponding treatment, cells were incubated with 5 μM Mag-Fluo-4-AM and 0.02% (w/v) Pluronic F-127 for 30 min at 37 °C in dark. Cd was removed by treatment of TPEN as described above. 488-nm laser was used to excite Mag-Fluo-4 fluorescence and $[Ca^{2+}]_{ER}$ was calculated by the fluorescence intensity (FL-1, 530 nm) of 10,000 cells on flow cytometer.

2.6. Determination of IP_3

Cells were plated in 100 mm culture dishes, then treated with 2.5 μM Cd when cell cultures reached 80–85% confluence. After 12 h treatment, cells were harvested, washed twice with a glucose-saline, PIPES buffer (pH 7.2, containing 25 mM PIPES, 110 mM NaCl, 5 mM KCl, 5.6 mM glucose, 0.4 mM $MgCl_2$, 0.1% BSA and 1 mM $CaCl_2$) and stimulated at 37 °C as indicated. The amount of IP_3 was determined according to the manufacturer's manual using a specific IP_3 [^{3}H] radioreceptor assay kit (Dupont NEN, Boston, USA). The lipid phase was counted to measure the phosphatidylinositol phosphate (PIP) lipid pool, except that the aqueous phase of the extract was passed through ultrafiltration units to exclude proteoglycans that interfere with the assay. IP_3 was expressed as a relative value of $(IP_3/PIP) \times 10^3$ (arbitrary units) to correct for the variation in the labelling of the lipid pool.

2.7. Western blotting analysis

Total protein lysates were obtained by lysing the cells with ice-cold RIPA buffer supplemented with protease inhibitors cocktail (Merck Millipore, Darmstadt, Germany). After protein quantification with BCA method, samples were subjected to SDS-PAGE gels and transferred to PVDF membranes. After blocking with 5% skim milk for 1 h at room temperature, membranes were incubated overnight at 4 °C with the following primary antibodies: IP_3R-1 (diluted 1:1000), IP_3R-2 (diluted

1:5000), p62 (diluted 1:1000), LC3B (diluted 1:1000) and β-actin (diluted 1:5000). Then membranes were washed in TBST for 30 min and incubated with appropriate secondary antibodies (1:5000 dilution) for 1 h at room temperature. Finally protein bands were detected on a Chemidoc XRS (Bio-Rad, Marnes-la-Coquette, France) by using the ECL Kit. Proteins levels were then determined by computer-assisted densitometric analysis (Densitometer, GS-800, BioRad Quantity One). The density of each band was normalized to its respective loading control (β-actin). Data obtained were expressed as the ratio of intensity of the protein in chemical-treated cells to that of the corresponding protein in control cells. Each test was performed in four experiments with different batches of cells.

2.8. Assessment of apoptosis by morphological changes and flow cytometry

BAPTA-AM (10 μM, cytosolic Ca^{2+} chelator), TG (1 μM, an inducer of ER-Ca^{2+} store depletion) and 2-APB (10 μM, an inhibitor of IP_3R) were applied to assess its effect on Cd-induced apoptosis, respectively. Apoptosis is characterized morphologically by condensation and fragmentation of nuclei. Therefore, Hoechst 33,258 staining was firstly applied to assess the morphological changes of treated cells, and 200 cells were randomly selected to count those apoptotic cells within every batch of experiment, each one performed in triplicate. Another concern is the quantitative analysis of apoptosis by flow cytometry. Both of these two methods have been extensively described in our previous study [22].

2.9. CCK-8 cell viability assay

Cell viability was performed using the CCK-8. Cells were seeded (4×10^3 per well) into 96-well plates and cultured for 48 h (about 80% confluence). Then cells were treated with three chemicals (BAPTA-AM, TG and 2-APB) and/or 2.5 μM Cd for 12 h as mentioned above. After a 12-h incubation, cell viability assays were performed using CCK-8, according to the manufacturers' instructions. The absorbance was measured at 450 nm by the microplate reader (Sunrise, Austria). All assays were performed in six independent experiments with different batches of cells.

2.10. Data presentation

Experiments were performed at least three times with similar results. Data are presented as the mean ± SEM of the indicated number of replicates. Statistical comparisons were made using one-way analysis of variance (ANOVA) (Scheffe's *F* test) after ascertaining the homogeneity of variance between the treatments, and $P < 0.05$ was regarded as significant.

3. Results

3.1. Elevated $[Ca^{2+}]_c$ was primarily generated intracellularly in Cd-exposed rPT cells

Our previous study has reported that cytosolic calcium overload occurred in Cd-treated rPT cells [13], but the source of Cd-induced $[Ca^{2+}]_c$ elevation, inside or outside of the cells, was not known. To clarify this issue, changes of $[Ca^{2+}]_c$ in Cd-treated rPT cells cultured in two media (Ca^{2+}-containing and Ca^{2+}-free) were measured by flow cytometer. It is worth noting that rPT cells are easy to detach from 6-well plates when they are incubated in CFM for >2 h (as we confirmed, data not shown). Thus, three different time points (0, 1, 2 h) was chosen to solve this question. Under normal culture conditions (Ca^{2+}-containing serum-free DMEM-F_{12} medium), 2.5 μM Cd-induced $[Ca^{2+}]_c$ exhibited a time-dependent elevation, i.e. 1.11-fold (1 h) and 1.16-fold (2 h) of its respective control value (Fig. 1A). Under Ca^{2+}-free medium conditions (Fig. 1B), there is also a time-dependent elevation in $[Ca^{2+}]_c$ exposed to 2.5 μM Cd, i.e., 1.07-fold (1 h) VS 1.14-fold (2 h). Data suggest that Cd-induced cytosolic calcium overload was primarily generated intracellularly and only a small portion was generated extracellularly.

3.2. Subcellular calcium redistribution occurred in Cd-exposed rPT cells

It is known that ER and mitochondria are two major intracellular Ca^{2+} stores. To verify whether Cd-induced $[Ca^{2+}]_c$ elevation resulted from these two Ca^{2+} stores, subcellular Ca^{2+} distribution in rPT cells exposed to 2.5 μM Cd was assessed by flow cytometer. Compared with samples in 0 h (no-Cd treatment), Cd-induced $[Ca^{2+}]_c$ elevation was accompanied by increased $[Ca^{2+}]_{mit}$ and decreased $[Ca^{2+}]_{ER}$ in a time-dependent manner (Fig. 2), and these changes were observed more obviously following 12-h Cd treatment.

3.3. Inhibition of ER Ca^{2+} release suppressed Cd-induced subcellular calcium redistribution

To investigate whether there is a link between ER Ca^{2+} release and Cd-elevated $[Ca^{2+}]_c$, cells were co-incubated with 2.5 μM Cd and/or 10 μM 2-APB (the blocker of ER Ca^{2+} release channel-IP_3R) for 12 h to determine the changes of $[Ca^{2+}]_c$, $[Ca^{2+}]_{mit}$ and $[Ca^{2+}]_{ER}$ using flow cytometer. As we expected, 2-APB significantly reversed Cd-induced ER Ca^{2+} depletion (Fig. 3A). Meanwhile, Cd-induced elevations in $[Ca^{2+}]_c$ and $[Ca^{2+}]_{mit}$ were significantly suppressed by the addition of 2-APB (Fig. 3B and C). Data in Fig. 3 suggested that depletion of ER Ca^{2+} stores plays a principal role in Cd-induced mobilization of Ca^{2+} in different cellular domains, i.e., Cd-induced $[Ca^{2+}]_c$ elevation was mainly originated from ER.

3.4. IP_3-initiated IP_3R activation is involved in Cd-exposed rPT cells

IP_3 is an important second messenger that induces the release of Ca^{2+} from the ER [23]. As shown in Fig. 4A, Cd led to the increased IP_3 production in rPT cells. Consequently, elevated IP_3 levels activate its receptor (IP_3R) in Cd-exposed rPT cells. We found that protein levels of IP_3R-1 (Fig. 4B) and IP_3R-2 (Fig. 4C) increased significantly in Cd-treated rPT cells. Particularly, the mRNA and protein expression of IP_3R-3 was not detectable in rPT cells (data not shown). Data in Fig. 4 validate that elevated IP_3 levels activated IP_3R to facilitate ER-Ca^{2+} release in Cd-exposed rPT cells.

3.5. Cd-inhibited autophagic flux was reversed by NAC treatment

The term “autophagic flux” is used to represent the dynamic process of autophagy, which is a more reliable indicator of autophagic activity than measurements of autophagosome numbers [6]. Compared with the control group, protein levels of p62 and LC3-II increased significantly in Cd-treated cells (Fig. 5A). CQ, a lysosome inhibitor, was used to block the autophagic flux in this study. As it is expected, treatment with 50 μM CQ alone induced the elevation of p62 and LC3-II. Likewise, Cd-induced p62 accumulation was further promoted by CQ treatment. However, no significant difference in LC3-II levels was observed between Cd-treated cells and cells exposed to Cd plus CQ. Taken together, these findings supported the notion that autophagic flux is decreased during Cd exposure.

The production of reactive oxygen species (ROS) is considered a major factor in Cd-induced nephrotoxicity. To clarify whether there is a link between ROS production and Cd-inhibited autophagic flux, NAC, a known ROS scavenger, was applied to prove this idea. As shown in Fig. 5B, 100 μM NAC treatment alone has no obvious effect on p62 and LC3-II protein levels, suggesting that it is not a modulator of autophagy. However, Cd-induced accumulation of p62 and LC3-II was significantly alleviated by NAC treatment, indicating that oxidative stress resulted in Cd-inhibited autophagic flux in rPT cells.

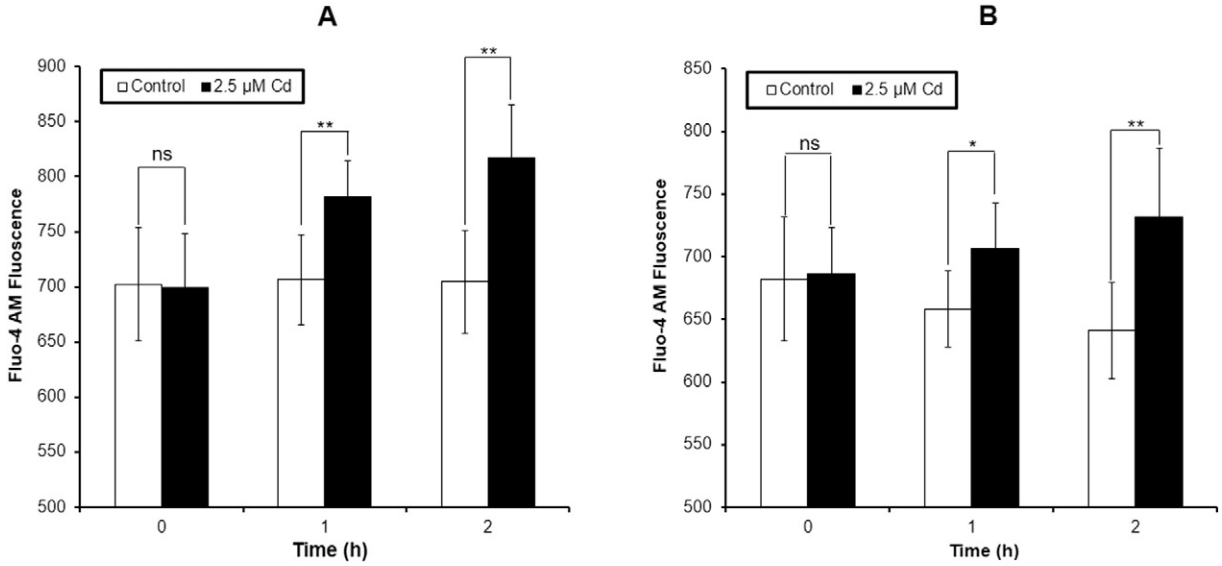

Fig. 1. Changes of cytosolic calcium levels ($[Ca^{2+}]_c$) in Cd-treated rPT cells cultured in Ca^{2+}-containing medium (A) and Ca^{2+}-free medium (B). Cells cultured in two different media were treated with 2.5 μM Cd for 0 h, 1 h and 2 h. The harvested cells were first incubated with 0.5 mM TPEN, then incubated with 1 μM Fluo-4/AM for 30 min at 37 °C to measure the Fluo-4 fluorescence using flow cytometer. Fluorescence results were expressed as mean fluorescence intensity. Data represent mean ± SEM ($n = 4$). *ns* not significant, $^{*}P < 0.05$, $^{**}P < 0.01$.

3.6. BAPTA-AM alleviated Cd-induced apoptosis and decrease of autophagic activity

To assess the role of intracellular Ca^{2+} in the connection between apoptosis and autophagy, BAPTA-AM, a cell permeable free calcium chelator, was chosen to investigate its effect on Cd-induced apoptosis and autophagic activity. We found that BAPTA-AM significantly prevented Cd-induced elevation of apoptosis, measured by two methods in rPT cells (Fig. 6A–C), while BAPTA-AM alone had no effect on it. Next, protein levels of p62 and LC3-II were determined by immunoblot assays. As shown in Fig. 6D, BAPTA-AM significantly reversed Cd-induced elevation of p62 and LC3-II protein levels, but BAPTA-AM treatment alone had no effect on both. These data suggested that intracellular calcium overload promoted apoptosis while inhibited autophagic flux in Cd-exposed rPT cells.

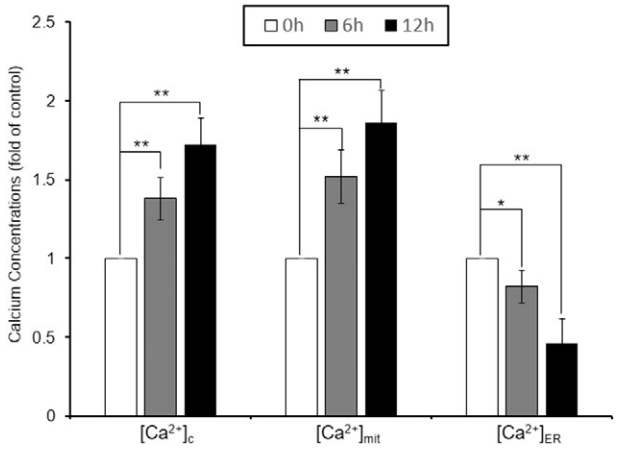

Fig. 2. Redistribution of calcium levels in the cytoplasm, mitochondria and ER occurred in Cd-exposed rPT cells. Cells were treated with 2.5 μM Cd for 0 h, 6 h and 12 h, then calcium levels in the cytoplasm ($[Ca^{2+}]_c$), mitochondria ($[Ca^{2+}]_{mit}$) and ER ($[Ca^{2+}]_{ER}$) were monitored by flow cytometric analysis, respectively. Samples of 0 h (Cd-free treatment) were assigned to the control groups. Values of fluorescence intensity of three calcium indicators are quantified in a relative way to its respective control, whose value of fluorescence intensity is set at one. Results represent mean ± SEM ($n = 6$). $^{*}P < 0.05$, $^{**}P < 0.01$.

3.7. TG aggravated Cd-mediated apoptosis and inhibition of autophagic flux

TG, an ER Ca^{2+} pump inhibitor, was used to deplete ER calcium stores in this study. Consequently, TG treatment alone caused significant cytosolic Ca^{2+} elevation and ER Ca^{2+} depletion in rPT cells (data not shown). As a positive control (up-regulator of $[Ca^{2+}]_c$), 1 μM TG alone markedly activated the apoptosis and inhibited the autophagic flux in rPT cells (Fig. 7). Moreover, Cd-induced apoptosis (morphological changes and apoptotic rates) and decreased autophagic flux were aggravated by TG treatment ($P < 0.01$), further verifying that elevated $[Ca^{2+}]_c$ played a dual role in regulating apoptosis and autophagy during Cd exposure.

3.8. 2-APB attenuated Cd-induced apoptosis and blockage of autophagic flux

2-APB, inhibitor of ER-Ca^{2+} release, was applied to investigate the role of ER-Ca^{2+} release in the process of apoptosis and autophagy during Cd exposure. Results of apoptotic morphological changes and flow cytometry analysis (Fig. 8A–C) showed that 10 μM 2-APB alone has no obvious effect on apoptosis, and it is not an autophagy regulator (Fig. 8D). However, 2-APB potently reversed Cd-induced apoptosis and accumulation of p62 and LC3-II in rPT cells, which highlighted that Cd-induced ER-Ca^{2+} release played an important role in the regulation of apoptosis and autophagic flux in rPT cells.

3.9. Regulators of Ca^{2+} signaling affected Cd-induced cytotoxicity

To further determine the role of subcellular Ca^{2+} redistribution on Cd-induced cytotoxicity in rPT cells, BAPTA-AM, TG and 2-APB was chosen to assess its effect on cell viability, respectively. As shown in Fig. 9, BAPTA-AM or 2-APB treatment alone had no significant toxic effect on cells, while TG alone exhibited significant cytotoxic effect on rPT cells. Cd-induced cytotoxicity was significantly alleviated by BAPTA-AM and aggravated by TG treatment, respectively; which evidenced that intracellular $[Ca^{2+}]_c$ elevation played a key role in cell death in Cd-exposed cells from both sides (pro/con). Moreover, 2-APB treatment markedly reversed Cd-induced cytotoxicity, further verifying that ER-Ca^{2+} release was a determinant in promoting Cd-induced cellular death.

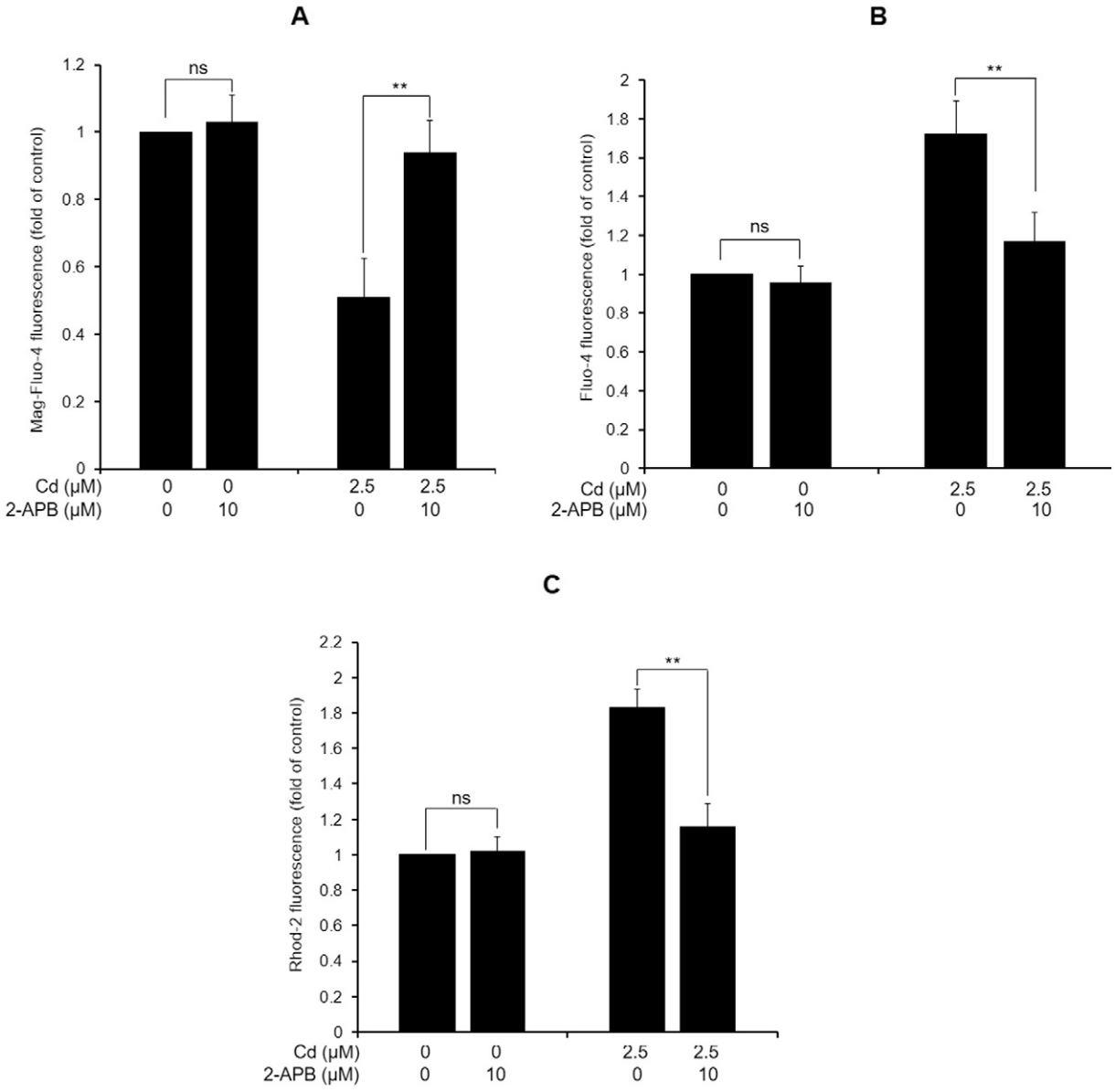

Fig. 3. 2-APB suppressed Cd-induced subcellular calcium distribution. Cells were co-incubated with 10 μM 2-APB and/or 2.5 μM Cd for 12 h to assess the changes of $[Ca^{2+}]_{ER}$ (A), $[Ca^{2+}]_c$ (B) and $[Ca^{2+}]_{mit}$ (C), assessed by flow cytometry. Values of fluorescence intensity of Mag-Fluo-4 (A), Fluo-4 (B) and Rhod-2 (C) are quantified in a relative way to its respective control, whose value is set at one. Data represent mean ± SEM ($n = 6$). *ns* not significant, $^{**}P < 0.01$.

4. Discussion

As previously reported, Cd-triggered apoptosis played a chief role in cell death in rPT cells, and elevation of $[Ca^{2+}]_c$ suggested that Ca^{2+} signaling may act as an important regulator during this process [13]. It is also well established that intracellular Ca^{2+} is one of the regulators of autophagy [24]. Herein, this study was designed to further systematically elucidate the source of Cd-induced $[Ca^{2+}]_c$ elevation and the regulatory role of intracellular Ca^{2+} overload in pathological connection between autophagy and apoptosis in Cd-exposed rPT cells.

Calcium is a versatile and dynamic second messenger that regulates numerous biological processes including apoptosis and autophagy [25,26]. Elevation of $[Ca^{2+}]_c$ is mediated by either Ca^{2+} influx from the extracellular medium or Ca^{2+} release from intracellular Ca^{2+} storage sites [27]. Where does Cd-induced $[Ca^{2+}]_c$ elevation originate from? Data in Fig. 1 suggest that Cd-elicited $[Ca^{2+}]_c$ elevation was primarily generated intracellularly and only a small portion was generated extracellularly. Thus, this study focused on the mechanism that how Cd affected subcellular Ca^{2+} distribution and its role in regulating apoptosis and autophagy. Cd-induced extracellular Ca^{2+} influx was not discussed here, which will be worthy of further investigation. Internal Ca^{2+} storages, such as ER and mitochondria, play a central role in maintaining intracellular calcium homeostasis [14]. So two specific Ca^{2+} probes targeting to mitochondria and ER, respectively, were employed to measure the changes of $[Ca^{2+}]_{mit}$ and $[Ca^{2+}]_{ER}$ in Cd-treated cells (Fig. 2). Elevated $[Ca^{2+}]_c$ was accompanied by elevated $[Ca^{2+}]_{mit}$ and decreased $[Ca^{2+}]_{ER}$, which enables us to think whether ER is the source of Cd-induced $[Ca^{2+}]_c$.

Ca^{2+} mobilization from the ER lumen is operated via two Ca^{2+} release channels: IP_3Rs and/or ryanodine receptors (RyRs) [28,29]. However, it is IP_3R rather than RyR that functioned as the Ca^{2+} release channel on ER membranes in rPT cells [30,31]. Thus, 2-APB, a specific inhibitor of IP_3R channel, was chosen to confirm the role of ER Ca^{2+} release in Cd-induced $[Ca^{2+}]_c$ elevation. As shown in Fig. 3, decreased $[Ca^{2+}]_{ER}$ was nearly completely reversed by 2-APB, providing evidence that Cd-induced ER Ca^{2+} depletion through activating IP_3R. Meanwhile, Cd-induced elevations in $[Ca^{2+}]_c$ and $[Ca^{2+}]_{mit}$ can be significantly reversed by 2-APB. Combined with data in Figs. 1 and 2, we can safely

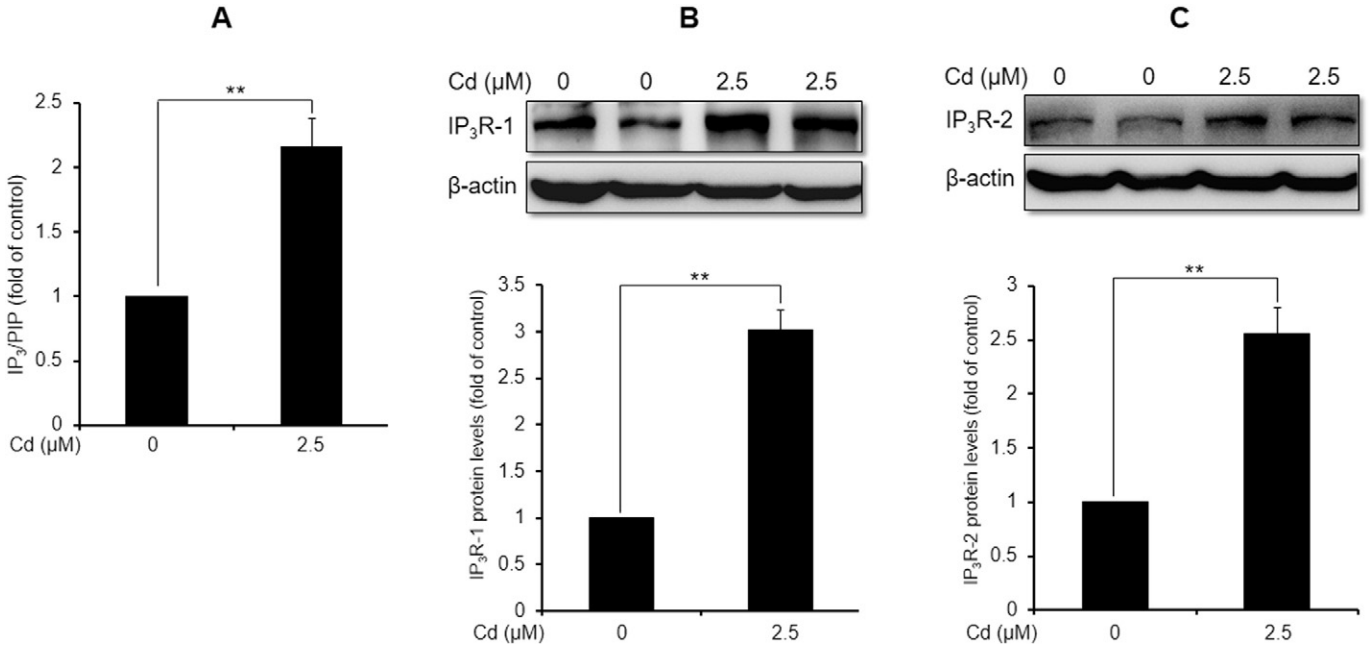

Fig. 4. Cd elevated the IP_3 levels and protein levels of IP_3R (IP_3R-1 and IP_3R-2) in rPT cells. (A) Cells were treated with 2.5 μM Cd for 12 h, then collected to measure the cellular IP_3 levels using a radio-receptor assay. Values represent mean ± SEM made in six different primary cultures ($n = 6$). (B, C) Cells were treated with 2.5 μM Cd for 12 h, then harvested to measure the protein levels of IP_3R-1 and IP_3R-2 using western blot. *Upper panel* representative western blot image; *lower panel* quantitative analysis (mean ± SEM, $n = 4$); $^{**}P < 0.01$.

draw the conclusion that Cd-elevated $[Ca^{2+}]_{mit}$ and $[Ca^{2+}]_c$ were mainly originated from IP_3R-mediated ER Ca^{2+} release, not from extracellular medium. Moreover, it is IP_3 that mobilized Ca^{2+} from ER to cytosol by binding and activating its specific receptors (IP_3Rs) localized on the ER membranes [32]. So, increased IP_3 generation (Fig. 4A) is the prerequisite for Cd-induced ER-Ca^{2+} release in rPT cells. There have been identified three subtypes of IP_3Rs (IP_3R-1, IP_3R-2 and IP_3R-3) differentially expressed in different regions of the kidney [33,34]. We have demonstrated that only the IP_3R-1 and IP_3R-2 isoforms are expressed in rPT cells [20]. In this study, Cd markedly up-regulated expressions of IP_3R-1 and IP_3R-2 (Fig. 4), indicating that activated IP_3R-1 and IP_3R-2 enhance both IP_3-binding sensitivity and ER Ca^{2+} release activity. Given the

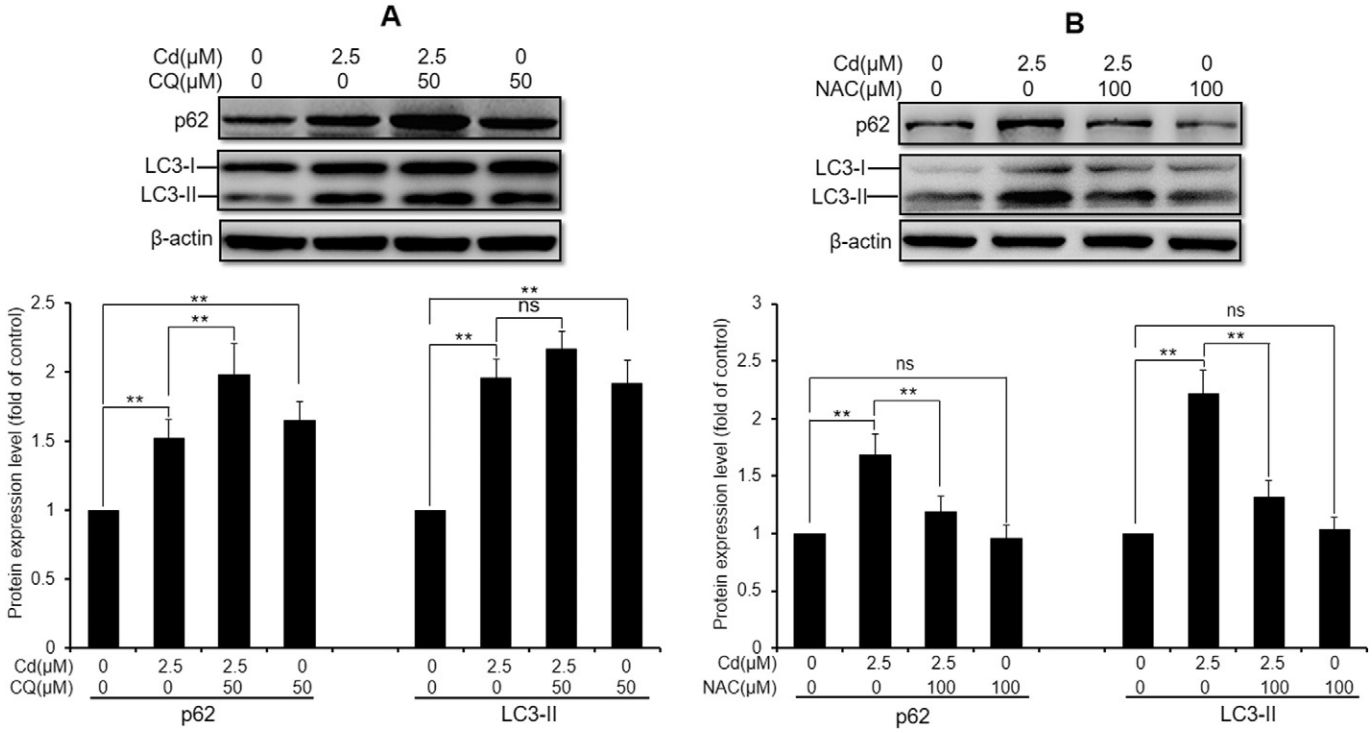

Fig. 5. Cd-inhibited autophagic flux can be alleviated by NAC treatment. (A) Cells were treated with 2.5 μM Cd for 9 h, subsequently co-incubated with 50 μM CQ for another 3 h. After 12 h treatment, cell were harvested to measure the protein levels of p62 and LC3-II using western blot. (B) Cells were co-incubated with 2.5 μM Cd and/or 100 μM NAC for 12 h, then harvested to assess the protein levels of p62 and LC3-II. *Upper panel* representative western blot image; *lower panel* quantitative analysis (mean ± SEM, $n = 4$); *ns* not significant, $^{**}P < 0.01$.

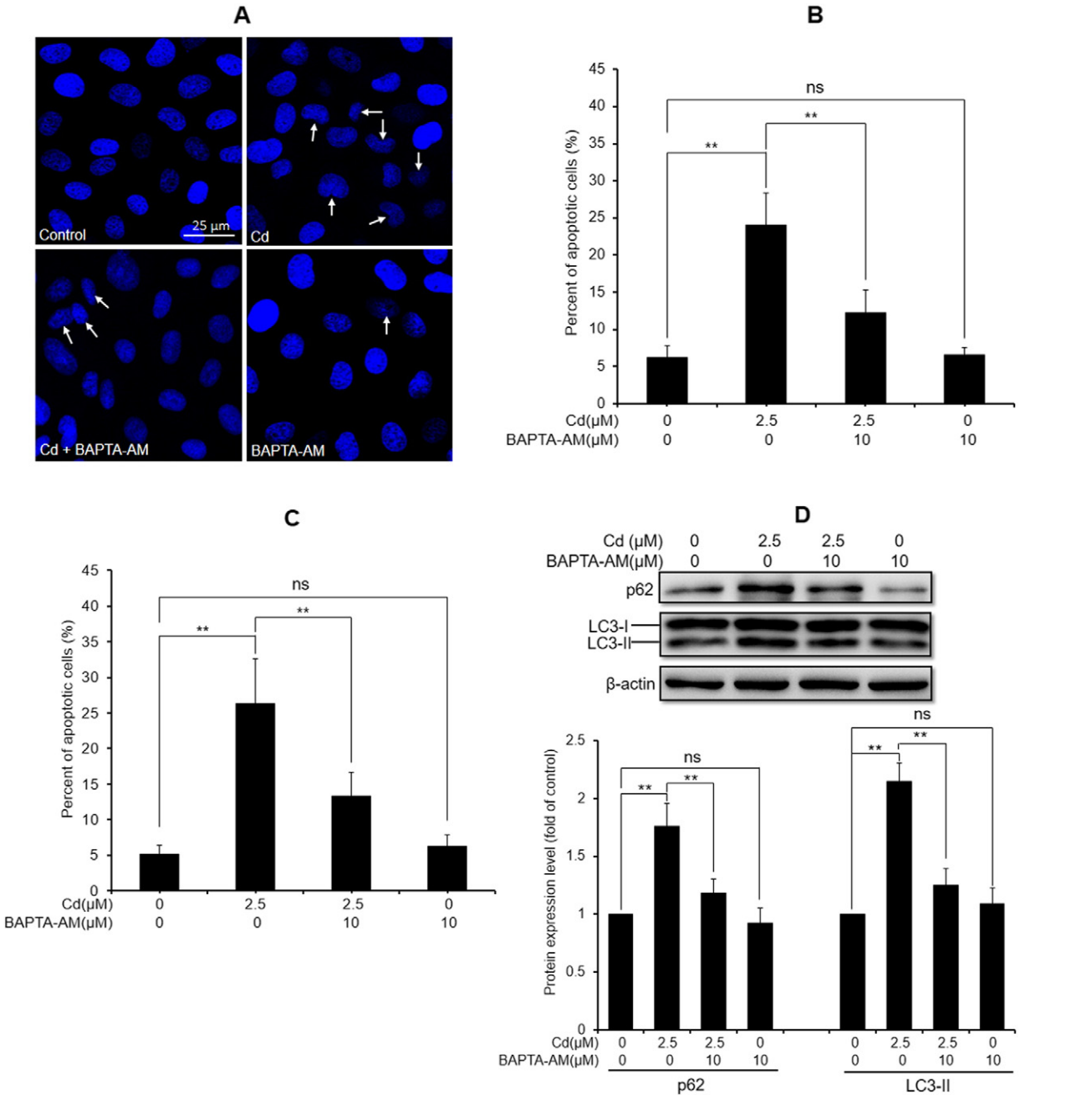

Fig. 6. Effect of BAPTA-AM on Cd-mediated apoptosis and autophagy. Cells were pretreated with 10 μM BAPTA-AM for 30 min, followed by treatment with 2.5 μM Cd for another 12 h. (A) Apoptotic morphological changes were assessed by Hoechst 33,258 staining. Changes of nuclei fragmentation with condensed chromatin are evident (thin arrows). (B) Quantitative analysis of apoptotic cells assessed by Hoechst 33,258 staining (mean ± SEM, $n = 9$). (C) Quantification of apoptosis using flow cytometer (mean ± SEM, $n = 6$). (D) Changes of p62 and LC3-II protein levels were analyzed by western blot. *Upper panel* representative western blot image; *lower panel* quantitative analysis (mean ± SEM, $n = 4$). *ns* not significant, $^{**}P < 0.01$.

above results, we can confirm that stimulated ER Ca^{2+} release resulting from the activation of IP_3Rs promoted the elevated $[Ca^{2+}]_c$ in Cd-exposed rPT cells.

Autophagy is an intracellular homeostatic mechanism important for the degradation of damaged organelles and undesirable macromolecules from the cytoplasm in acidic lysosomal compartments [35]. Immunoblot analysis of LC3 and p62 has been widely used to monitor autophagic flux [7,36]. LC3 conversion (LC3-I to LC3-II) and lysosomal degradation of LC3-II reflect the progression of autophagy. Importantly, LC3-II turnover assay in the presence of the lysosomal inhibitor was a known method to assess autophagic flux [6]. Meanwhile, the p62 protein level is inversely correlated with autophagic activity and increased p62 is a reliable indicator of impaired autophagic flux [6]. Given the above mentioned, the autophagic flux was impaired in Cd-exposed rPT cells, as evidenced from data in Fig. 5A. Mounting evidence suggests that autophagy and oxidative stress are intricately connected in kidney health and disease [37]. Moreover, it has been confirmed that oxidative stress-mediated apoptotic death played a key role in Cd-induced nephrotoxicity in vitro, which prompted us to think whether there is a link between impaired autophagic flux and oxidative stress during Cd exposure. Data in Fig. 5B showed that Cd-induced impairment of autophagic flux was markedly restored by the addition of NAC (a known ROS scavenger), demonstrating that impaired autophagic flux results from oxidative stress in this process.

Disruption of intracellular Ca^{2+} homeostasis can lead to cellular death [38]. It has been revealed that cytosolic Ca^{2+} overload can trigger

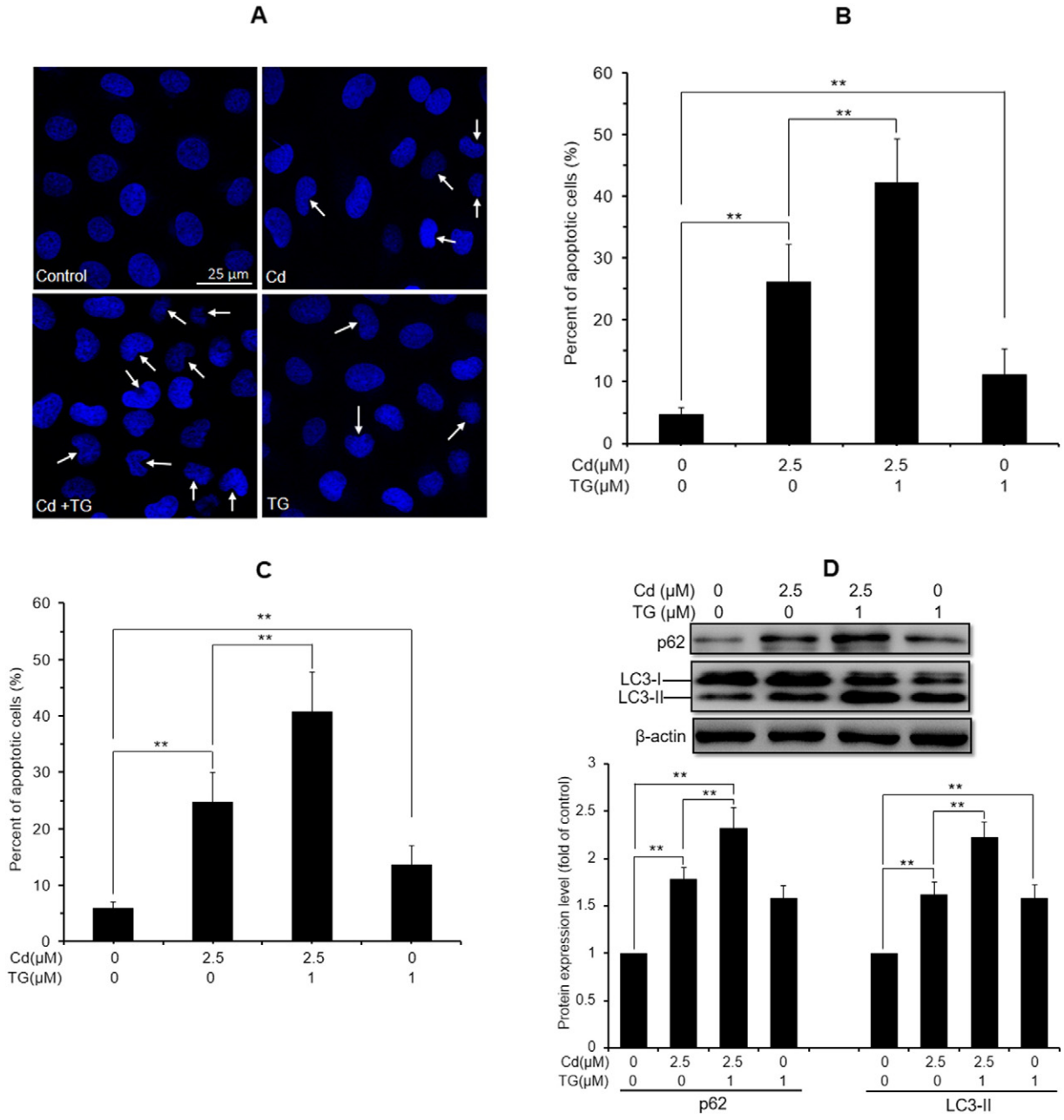

Fig. 7. TG aggravated Cd-mediated apoptosis and inhibition of autophagic flux. Cells were co-treated with 1 μM TG and/or 2.5 μM Cd for 12 h. Apoptotic morphological changes were assessed by Hoechst 33,258 staining (A) and its statistical result of apoptotic cells (B) are expressed as mean ± SEM ($n = 9$). (C) Quantification of apoptosis using flow cytometer (mean ± SEM, $n = 6$). (D) Changes of p62 and LC3-II protein levels were analyzed by western blot. *Upper panel* representative western blot image; *lower panel* quantitative analysis (mean ± SEM, $n = 4$). $^{**}P < 0.01$.

apoptosis [14], but controversial idea has been present in the role of $[Ca^{2+}]_c$ elevation in regulating autophagy, with both activating and inhibitory effects [39,40]. Our previous study proved that Cd-mediated apoptosis is accompanied by cytosolic Ca^{2+} overload, which gives us a hint that whether $[Ca^{2+}]_c$ elevation serves as a link between apoptosis and autophagic flux inhibition. Hereby, pharmacological agents that regulate cytosolic Ca^{2+} level were applied to clarify this question. Firstly, blocking $[Ca^{2+}]_c$ elevation by intracellular Ca^{2+} chelator (BAPTA-AM) effectively attenuated Cd-induced apoptosis and autophagic flux inhibition (Fig. 6); moreover, TG, which can induce $[Ca^{2+}]_{ER}$ depletion and $[Ca^{2+}]_c$ elevation [41], further aggravated Cd-mediated apoptosis and autophagic flux impairment (Fig. 7), confirming that Cd induces autophagy inhibition and apoptosis through elevation of $[Ca^{2+}]_c$ in rPT cells from both sides (pro/con). Consistent with our findings, Park et al. (2014) reported that a chronic increased $[Ca^{2+}]_c$ in hepatocytes during lipotoxicity attenuates autophagic flux by preventing the fusion between autophagosomes and lysosomes [42]. Data in Fig. 7 also showed that ER-Ca^{2+} release plays a positive regulator during this process. Similarly, evidence has shown that IP_3Rs act as inhibitors of autophagy because knocking down IP_3Rs or inhibiting its channel activity by 2-APB was sufficient to induce conversion of LC3-I to LC3-II [26]. Consistent with this idea, we observed that inhibition of IP_3Rs by 2-APB to abolish ER Ca^{2+} release significantly reversed Cd-induced apoptosis and autophagy flux inhibition (Fig. 8). It is also known that disturbance of the ER Ca^{2+} homeostasis leads to extensive and irreparable damage to cells [17], thus data in Fig. 9 verified the role of Ca^{2+} signaling in the regulation of Cd-induced cytotoxicity.

In summary, Cd induced an subcellular calcium redistribution in rPT cells, i.e., elevations of $[Ca^{2+}]_c$, $[Ca^{2+}]_{mit}$ and decreased $[Ca^{2+}]_{ER}$. Stimulated ER Ca^{2+} release due to the activation of IP_3Rs is responsible for

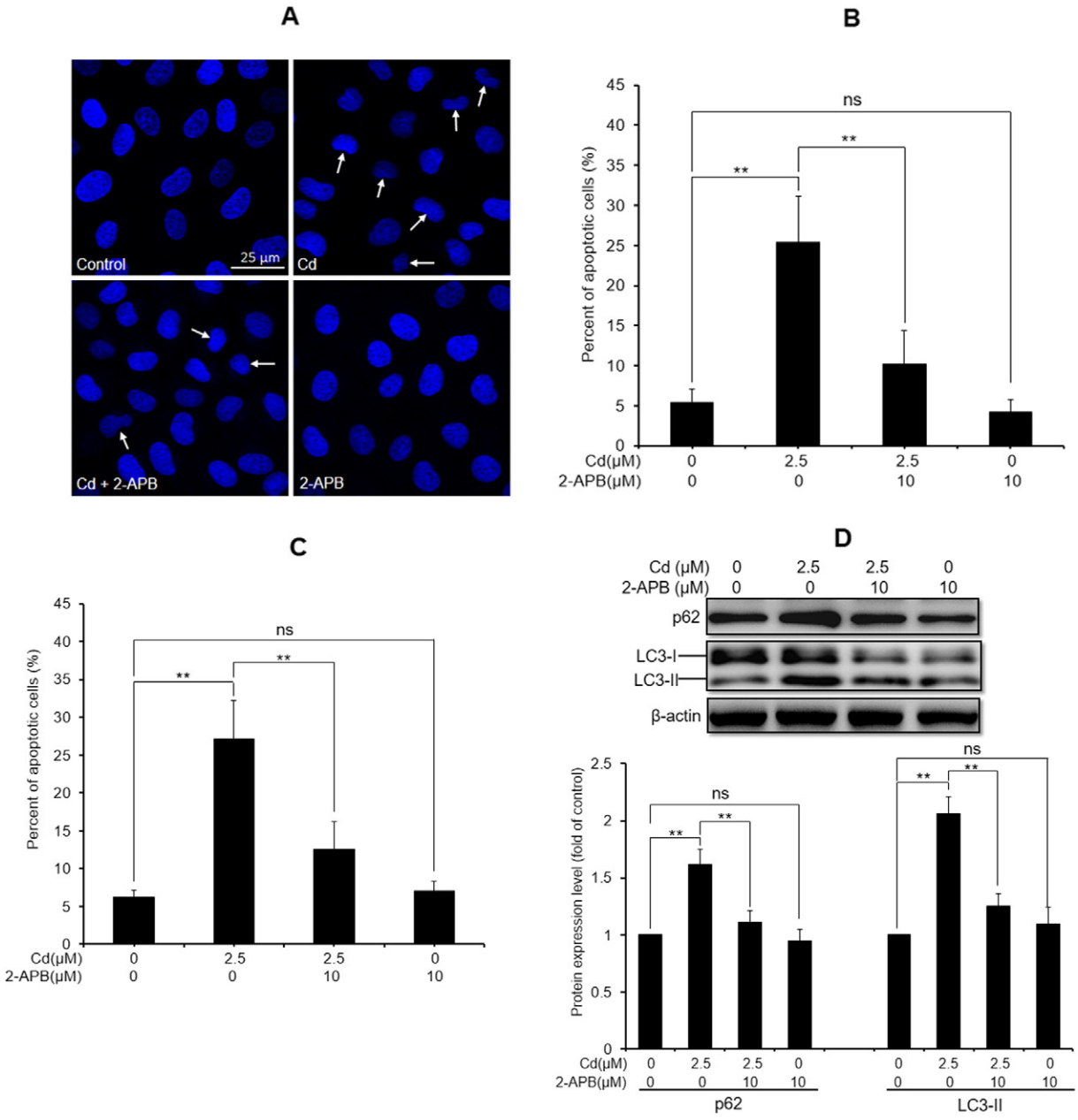

Fig. 8. 2-APB alleviated Cd-induced apoptosis and blockage of autophagic flux. Cells were co-incubated with 10 μM 2-APB and/or 2.5 μM Cd for 12 h. Apoptotic morphological changes were assessed by Hoechst 33,258 staining (A) and its statistical result of apoptotic cells (B) are expressed as mean ± SEM ($n = 9$). (C) Quantification of apoptosis using flow cytometer (mean ± SEM, $n = 6$). (D) Changes of p62 and LC3-II protein levels were analyzed by western blot. *Upper panel* representative western blot image; *lower panel* quantitative analysis (mean ± SEM, $n = 4$). *ns* not significant, $^{**}P < 0.01$.

the increase in $[Ca^{2+}]_c$. Furthermore, elevated $[Ca^{2+}]_c$ can promote apoptosis and suppress autophagic flux, demonstrating that disturbance in intracellular Ca^{2+} signaling regulated by ER plays a dual role in Cd-induced cytotoxicity in rPT cells.

5. Abbreviations

2-APB	2-aminoethoxydiphenyl borate
BAPTA-AM	1,2-Bis (2-aminophenoxy) ethane-*N*,*N*,*N*′,*N*′-tetraacetic acid acetoxymethyl ester
BCA	bicinchonininc acid
$[Ca^{2+}]_c$	cytosolic Ca^{2+} concentration
$[Ca^{2+}]_{ER}$	endoplasmic reticulum Ca^{2+} levels
$[Ca^{2+}]_{mit}$	mitochondrial Ca^{2+} concentration
CCK-8	Cell Counting Kit-8
Cd	cadmium
CFM	calcium-free medium
CQ	chloroquine diphosphate salt
ECL	enhanced chemiluminescence
ER	endoplasmic reticulum
IP_3	inositol 1,4,5-trisphosphate
IP_3R	IP_3 receptor
LC3	microtubule-associated protein 1 light chain 3
NAC	*N*-acetylcysteine
P62/SQSTM1	sequestosome 1
PI	propidium iodide
PIP	phosphatidylinositol phosphate
rPT	rat proximal tubular
ROS	reactive oxygen species
TG	thapsigargin

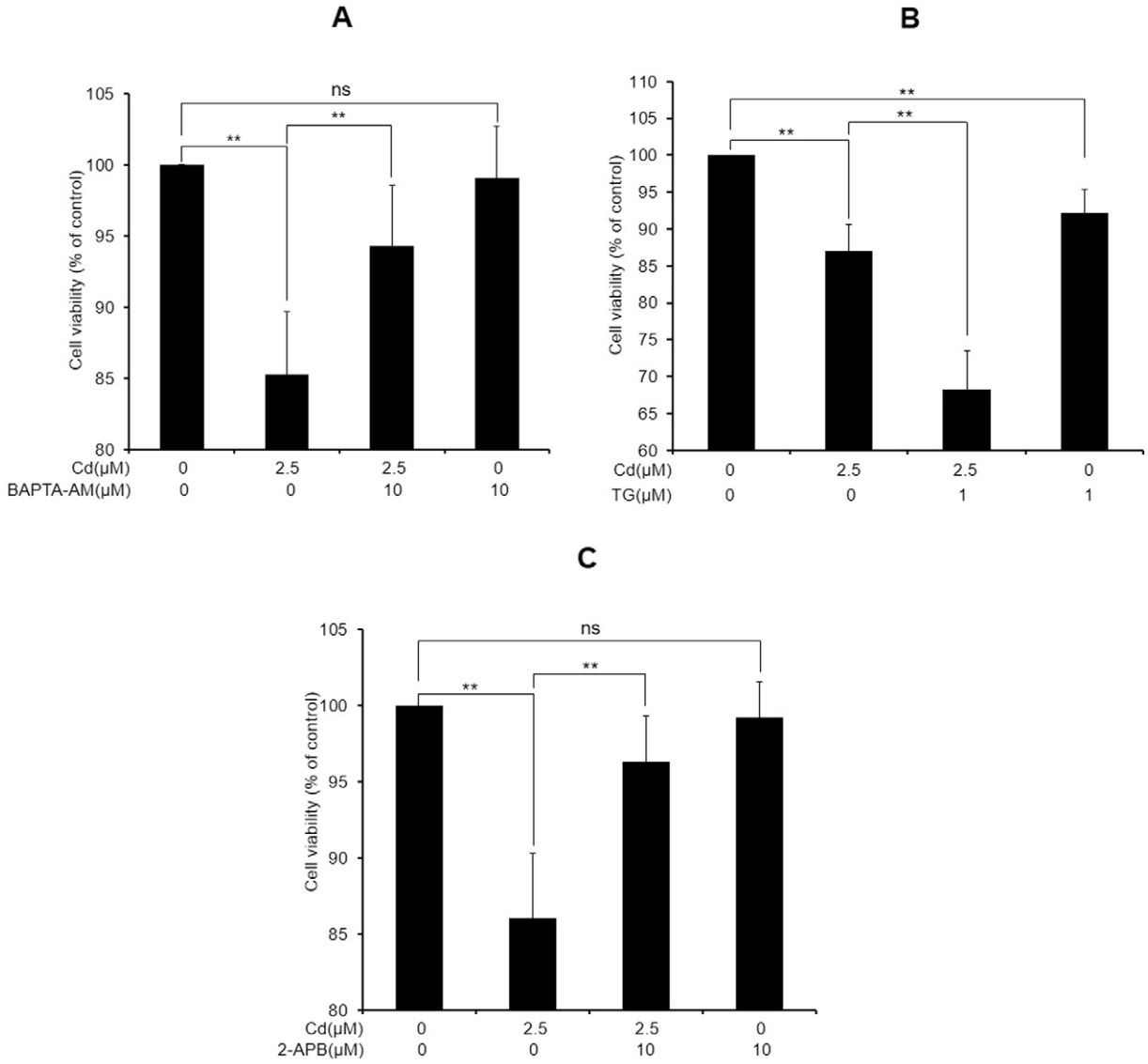

Fig. 9. Effects of three Ca^{2+} signaling regulators on Cd-induced cytotoxicity. Cells were treated with 10 μM BAPTA-AM, 1 μM TG, 10 μM 2-APB and/or 2.5 μM Cd as mentioned above, respectively. After a 12-h treatment, cell viability assays were measured by CCK-8 reduction method. Cell viabilities of the respective control group were assumed as 100% and the variations were represented as percentage. Data are expressed as mean ± SEM ($n = 6$).

TPEN *N,N,N′,N′*-tetrakis-(2-pyridylmethyl) ethylenediamine

Conflict of interest

None declared.

Acknowledgements

This work was supported by the National Natural Science Foundation of China (NSFC) (No. 31472251), a Foundation for the Author of National Excellent Doctoral Dissertation of PR China (No. 201266) and the fund of Fok Ying Tung Education Foundation under Grant No. 141022.

References

[1] P.B. Tchounwou, C.G. Yedjou, A.K. Sutton, D.J. Patlolla, EXS 101 (2012) 133–164.
[2] M. Waisberg, P. Joseph, B. Hale, D. Beyersmann, Toxicology 192 (2003) 95–117.
[3] N. Johri, G. Jacquillet, R. Unwin, Biometals 23 (2010) 783–792.
[4] H.C. Gonick, Indian J. Med. Res. 128 (2008) 335–352.
[5] W.C. Prozialeck, A. VanDreel, C.D. Ackerman, I. Stock, A. Papaeliou, C. Yasmine, K. Wilson, P.C. Lamar, V.L. Sears, J.Z. Gasiorowski, K.M. DiNovo, V.S. Vaidya, J.R. Edwards, Biometals 29 (2016) 131–146.
[6] N. Mizushima, T. Yoshimori, B. Levine, Cell 140 (2010) 313–326.
[7] D.J. Klionsky, K. Abdelmohsen, A. Abe, et al., Autophagy 12 (2016) 1–222.
[8] O. Lenoir, P.L. Tharaux, T.B. Huber, Kidney Int. pii: S0085-2538(16)30173-9 (2016, Jun 18) S0085-2538, http://dx.doi.org/10.1016/j.kint.2016.04.014 [Epub ahead of print].
[9] A. Kimura, Y. Ishida, M. Nosaka, Y. Kuninaka, M. Hama, T. Kawaguchi, S. Sakamoto, K. Shinozaki, Y. Iwahashi, T. Takayasu, T. Kondo, Toxicology 339 (2016) 9–18.
[10] A.R. Nair, W.K. Lee, K. Smeets, Q. Swennen, A. Sanchez, F. Thévenod, A. Cuypers, Arch. Toxicol. 89 (2015) 2273–2289.
[11] L. Liu, B. Yang, Y. Cheng, H. Lin, Biol. Trace Elem. Res. 167 (2015) 308–319.
[12] M. Erboga, M. Kanter, C. Aktas, U. Sener, Z. Fidanol-Erboga, Y. Bozdemir-Donmez, A. Gurel, Biol. Trace Elem. Res. 170 (2016) 165–172.
[13] L. Wang, J. Cao, D. Chen, X. Liu, H. Lu, Z. Liu, Biol. Trace Elem. Res. 127 (2009) 53–68.
[14] S.S. Smaili, G.J. Pereira, M.M. Costa, K.K. Rocha, L. Rodrigues, L.G. do-Carmo, H. Hirata, Y.T. Hsu, Curr. Mol. Med. 13 (2013) 252–265.
[15] H. Du, L. Liu, L. You, M. Yang, Y. He, X. Li, L. Xiong, Plant Mol. Biol. 77 (2011) 47–63.
[16] J.P. Decuypere, J.B. Parys, G. Bultynck, Autophagy 11 (2015) 1944–1948.
[17] S.H. Wang, Y.L. Shih, W.C. Ko, Y.H. Wei, C.M. Shih, Cell. Mol. Life Sci. 65 (2008) 3640–3652.
[18] G. Liu, Z.K. Wang, Z.Y. Wang, D.B. Yang, Z.P. Liu, L. Wang, Arch. Toxicol. 90 (2016) 1193–1209.
[19] T. Takenouchi, K. Ogihara, M. Sato, H. Kitani, Biochim. Biophys. Acta 15 (2005) 177–186.
[20] H. Wang, Z.K. Wang, P. Jiao, X.P. Zhou, D.B. Yang, Z.Y. Wang, L. Wang, Toxicology 333 (2015) 137–146.
[21] R. Fukumori, T. Takarada, N. Nakamichi, Y. Kambe, H. Kawagoe, R. Nakazato, Y. Yoneda, Neurochem. Int. 57 (2010) 730–737.

[22] L. Wang, H. Wang, M. Hu, J. Cao, D. Chen, Z. Liu, Arch. Toxicol. 83 (2009) 417–427.
[23] K. Mikoshiba, J. Neurochem. 102 (2007) 1426–1446.
[24] J.P. Decuypere, G. Bultynck, J.B. Parys, Cell Calcium 50 (2011) 242–250.
[25] C.J. Hanson, M.D. Bootman, H.L. Roderick, Curr. Biol. 14 (2004) 933–935.
[26] M.W. Harr, C.W. Distelhorst, Cold Spring Harb. Perspect. Biol 2 (10) (2010) a005579, http://dx.doi.org/10.1101/cshperspect.a005579.
[27] K. Bianchi, G. Vandecasteele, C. Carli, A. Romagnoli, G. Szabadkai, R. Rizzuto, Cell Death Differ. 13 (2006) 586–596.
[28] D.S. Luciani, K.S. Gwiazda, T.L. Yang, T.B. Kalynyak, Y. Bychkivska, M.H. Frey, K.D. Jeffrey, A.V. Sampaio, T.M. Underhill, J.D. Johnson, Diabetes 58 (2009) 422–432.
[29] M.D. Seo, M. Enomoto, N. Ishiyama, P.B. Stathopulos, M. Ikura, Biochim. Biophys. Acta 1853 (2015) 1980–1991.
[30] O. Aizman, P. Uhlén, M. Lal, H. Brismar, A. Aperia, Ouabain, Proc. Natl. Acad. Sci. U. S. A. 98 (2001) 13420–13424.
[31] J. Li, S. Zelenin, A. Aperia, O. Aizman, J. Am. Soc. Nephrol. 17 (2006) 1848–1857.
[32] C.J. Stork, Y.V. Li, J. Mol. Signal. 5 (2010) 5.
[33] I. Fujino, N. Yamada, A. Miyawaki, M. Hasegawa, T. Furuichi, K. Mikoshiba, Cell Tissue Res. 280 (1995) 201–210.
[34] T. Fujimoto, S. Shirasama, Int. J. Mol. Med. 30 (2012) 1287–1293.
[35] D.J. Puleston, A.K. Simon, Immunology 141 (2014) 1–8.
[36] P. Jiang, N. Mizushima, Methods 75 (2015) 13–18.
[37] A. Sureshbabu, S.W. Ryter, M.E. Choi, Redox Biol. 4 (2015) 208–214.
[38] M. Shi, T. Zhang, L. Sun, Y. Luo, D.H. Liu, S.T. Xie, X.Y. Song, G.F. Wang, X.L. Chen, B.C. Zhou, Y.Z. Zhang, Apoptosis 18 (2013) 435–451.
[39] P.B. Gordon, I. Holen, M. Fosse, J.S. Røtnes, P.O. Seglen, J. Biol. Chem. 268 (1993) 26107–26112.
[40] C. Cárdenas, J.K. Foskett, Cell Calcium 52 (2012) 44–51.
[41] F. Michelangeli, J.M. East, Biochem. Soc. Trans. 39 (2011) 789–799.
[42] H.W. Park, H. Park, I.A. Semple, I. Jang, S.H. Ro, M. Kim, V.A. Cazares, E.L. Stuenkel, J.J. Kim, J.S. Kim, J.H. Lee, Nat. Commun. 5 (2014) 5834.